

UIIU-ENG 86-3601

Report No. 124

ESTIMATING THE EFFECTS OF RESIDUAL STRESS
ON THE FATIGUE LIFE OF NOTCHED COMPONENTS

by

F. V. Lawrence, Jr. and J.-Y. Yung
Departments of Civil Engineering and Metallurgy

A Report of the
MATERIALS ENGINEERING - MECHANICAL BEHAVIOR
College of Engineering, University of Illinois at Urbana-Champaign
April 1986

TABLE OF CONTENTS

1. INTRODUCTION
2. ESTIMATING THE FATIGUE CRACK INITIATION LIFE (N_I)
 - 2.1 Defining the Stress History (Task 1)
 - 2.2 Determining the Effects of Geometry (Task 2)
 - 2.3 Estimating the Residual Stresses (Task 3)
 - 2.4 Material Properties (Tasks 4 - 6)
 - 2.5 Estimating the Fatigue Notch Factor (Task 7)
3. THE SET-UP CYCLE (TASK 8)
4. THE DAMAGE ANALYSIS (TASK 10)
 - 4.1 Predicting the Fatigue Behavior under Constant Amplitude Loading with No Notch-Root Yielding or Mean-Stress Relaxation
 - 4.2 Predicting the Fatigue Behavior under Constant Amplitude Loading with Notch-Root Yielding and No Mean-Stress Relaxation
 - 4.3 Predicting the Fatigue Crack Initiation Life under Constant Amplitude Loading with Notch-Root Yielding and Mean-Stress Relaxation
 - 4.4 Predicting the Fatigue Crack Initiation Life under Variable Load Histories without Mean Stress Relaxation

FIGURES

APPENDIX: ESTIMATING THE FATIGUE LIFE DEVOTED TO CRACK PROPAGATION (N_p)

REFERENCES

LIST OF FIGURES

- Fig. 1 Schematic diagram for the fatigue crack initiation life estimation procedure.
- Fig. 2 The location of strain gages relative to the notch and the separation of remote axial and bending strains (stresses).
- Fig. 3 (a) Finite element mesh for T joints subjected to bending and shear; (b) contours of tensile maximum principal stresses resulting from (a).
- Fig. 4 Yield strength as a function of ultimate strength and hardness [7].
- Fig. 5 Fatigue strength coefficient as a function of ultimate strength and hardness [7].
- Fig. 6 Relaxation exponent as a function of plastic strain amplitude [1,8].
- Fig. 7 Peened material hardness as a function of base metal hardness [9].
- Fig. 8 Heat-affected-zone hardness as a function of base metal hardness [7].
- Fig. 9 Elastic stress concentration factor (K_t) and fatigue notch factor (K_f) as a function of toe root radius. K_{fmax} is the "worst case" value of K_f for a given material and geometry.
- Fig. 10 Set-up cycle analysis for the weld toe with tensile residual stresses. Note the change of the sign of the notch-root residual stresses after the second reversal of load.
- Fig. 11 Set-up cycle for ASTM A514 HAZ (strong), A36 HAZ (tough) steels, and aluminum alloy 5183 WM (ductile) materials [11]. The set-up cycle may eliminate notch-root residual stresses in ductile materials.
- Fig. 12 Reversal of sign of residual stresses after set-up cycle. An example of compressive loadings and compressive residual stresses.
- Fig. 13 Comparison of fatigue strength predicted using Eq. 14 with experimental data [9].
- Fig. 14 Use of the proposed nomograph for the fatigue design of as-welded ASTM A36 steel weldments [5].
- Fig. 15 Nomograph for the fatigue design of stress-relieved ASTM A36 weldments [5].
- Fig. 16 Nomograph for the fatigue design of shot-peened ASTM A36 weldments [5].
- Fig. 17 Mean stress relaxation behavior as a function of cycles [11].

- Fig. 18 Mean stress relaxation influence on the fatigue crack initiation life [11].
- Fig. A1 (a) Longitudinal residual stress field due to welding (hatched area: weld metal);
(b) Crack in residual stress field [17].
- Fig. A2 (a) Typical residual stress distributions resulting from shot-peening [18];
(b) Hypothetical notch residual distributions and corresponding residual stress intensity factors [21,22].

ESTIMATING THE EFFECTS OF RESIDUAL STRESS
ON THE FATIGUE LIFE OF NOTCHED COMPONENTS

F.V. Lawrence, Jr.
J.-Y. Yung

1. INTRODUCTION

There are four important attributes of notched components which together with the magnitude of the fluctuating stresses applied, determine their resistance to metallic fatigue: the ratio of the axial and the applied or self-induced bending stresses; the severity of the notch or discontinuity; the notch-root residual stresses which result from fabrication, post-fabrication treatment or subsequent use; and the mechanical properties of the notch-root material in which the fatigue crack initiation and growth takes place. In this review, the application of an analytical model for predicting the fatigue behavior of notched components will be discussed with emphasis given to estimating the effects of residual stresses.

The authors and their coworkers have developed a model for the fatigue life of weldments which can be applied quite generally to estimate the fatigue resistance of notched components [1]. This model considers the total fatigue life (N_T) to be comprised of a period devoted to crack initiation and early growth (N_I) and a period devoted to the growth of a dominant crack (N_P). While the total life is the sum of these two periods, at long lives, N_I dominates [1,2] and the fatigue life or fatigue strength of a notched member can be estimated by considering only crack initiation and early growth through the Basquin equation with the Morrow mean stress correction:

$$\sigma_a = (\sigma_f' - \sigma_m)(2N_I)^b \quad (1)$$

where σ_a is the stress amplitude, σ_f' is the fatigue strength coefficient, σ_m is the mean stress which includes the residual and local mean stress after the first cycle of load (set-up cycle), $2N_I$ is the reversals devoted to crack initiation and early growth (one cycle equals two reversals) and b is the fatigue strength coefficient.

The general scheme for estimating N_I is diagrammed in Fig. 1. Estimates of the total fatigue life (N_T) can be obtained by adding the crack

propagation life (N_p) to these estimates of N_I . A method of estimating the effects of residual stresses on the crack propagation life (N_p) is summarized in the Appendix. The intent of the remainder of this review is to give a step-by-step summary of the authors' method of estimating the fatigue crack initiation life N_I using the schematic diagram of Fig. 1 as a guide.

2. ESTIMATING THE FATIGUE CRACK INITIATION LIFE (N_I)

The steps in the estimation of the fatigue crack initiation life (N_I) are diagrammed in Fig. 1. Each step in the analysis is numbered in the approximate sequence in which it is carried out. At the left are four main types of information which must be collected, estimated (or guessed) to permit the calculation of the long life fatigue strength or fatigue crack initiation life (N_I): one requires information about the service history, notch and loading geometry, residual stresses, and notch-root material properties. The accuracy of the predictions to be made depends most sensitively upon the level and nature of the applied stresses (Task 1). The effects of geometry can be calculated with considerable accuracy (Task 2) and the appropriate values for the residual stresses (Task 3) and particularly the material properties (Tasks 4-6) can usually be roughly estimated without greatly diminishing the accuracy of the calculation.

Having collected this information and used it to estimate the fatigue notch factor (Task 7) and, if necessary, the stress relaxation constant (Task 9), two main analyses are then carried out: the Set-up Cycle analysis (Task 8) and the Damage Summation analysis (Task 10).

2.1 Defining the Stress History (Task 1)

The most important step in the estimation of N_I is determining the nominal stresses in the vicinity of the critical notch (Task 1). Indeed, the entire analysis depends on identifying the critical notch or notches and determining the stresses in their vicinity. In the case of weldments, one applies strain gages near the weldment and measures the nominal axial and bending strains (Fig. 2). It is important to partition the bending and axial stresses since the elastic stress concentration factors, K_t (Task 2) and consequently K_f determined in Task 7 are different for these two types of stresses.

Proper gage placement may require a stress analysis of the notch and its vicinity to identify areas in which the global stresses can be measured without entering the stress field of the notch itself and consequently making the measured strains an essentially unknown function of gage placement. Global stress analyses which give strain-gage accuracy should provide adequate information in the absence of a prototype and the possibility of measuring strain directly.

In bi-axial loading cases, the nominal maximum principal stresses should be determined [3]. If the load history cannot be considered to be constant amplitude, then the load history must be recorded and edited for subsequent use in Tasks 8 and 10.

2.2 Determining the Effects of Geometry (Task 2)

The fatigue process usually occurs at notches. Thus, it is necessary to quantify the severity of the critical notch using a parameter which describes the intensification of stress at the notch root during the set-up and subsequent cycles, the fatigue notch factor K_f . The fatigue notch factor is equal to or less than the elastic stress concentration factor K_t . The factor K_t can be analytically determined using finite element stress analysis methods (Task 2) and can be used to estimate K_f (Task 7) using Peterson's equation:

$$K_f = 1 + (K_t - 1)/(1 + a/r) \quad (2)$$

The K_t of many notches have been collected by Peterson [4]. The stress concentration factor of complex notches can be estimated using finite element stress analysis methods. Such stress analyses determine both the notch-root stresses (which control the crack initiation and early growth phenomena) and the variation of stresses along the crack path away from the notch root (which determines the variation of stress intensity factor (ΔK_I) with crack depth and hence the rate of fatigue crack propagation or N_p ; see the Appendix).

Our practice has been to establish a definite radius at the notch root and to refine the element size to an order of magnitude less than this radius: see Fig. 3. Values of K_t for radii smaller or larger than that used in the analysis can be estimated in many cases by the expression:

$$K_t = 1 + \alpha(t/r)^{1/2} \quad (3)$$

where α is a coefficient which describes the severity of the notch, r is the notch root radius and t is a measure of the size of the component (plate thickness or shaft diameter, etc.). Because the stress concentration factor for purely axial loads is different and usually greater than that for pure bending, finite element analyses must be carried out for both the axial and bending cases, and values of K_t and α must be determined for each. A summary of axial and bending K_t values for common weld shapes is given in [5].

2.3 Estimating the Residual Stresses (Task 3)

After the magnitude of the applied stress, the notch-root residual stresses are the most influential factor in determining the fatigue resistance of notched components of a given material. The notch root residual stresses are generally unknown and difficult to measure; consequently, estimating the value of the notch root residual stresses is very important. Fortunately, obtaining estimates of sufficient accuracy is facilitated by several facts: first, the level of notch-root residual stress is often greatly altered during the set-up cycle (Task 8) so that the value of the notch-root residual stress may not depend too heavily upon its initial value prior to the set-up cycle but rather upon the set-up cycle itself; secondly, under high strain amplitudes, the notch-root residual stresses may quickly relax or shake down to negligible values; thirdly, the initial value of residual stress can often be bounded by the ability of the material to sustain residual stresses, so that, as in the case of weldments, one can adopt the pessimistic view that the residual stresses are as large as possible, that is, limited only by the yield strength of the (base) metal.

We therefore customarily assume that the initial value of residual stress is:

$$\begin{aligned} \sigma_r &= S_y && \text{for weldments in the as welded state, etc.} \\ \sigma_r &= 0 && \text{for stress-relieved or residual stress free conditions} \\ \sigma_r &= -S_y && \text{for peened or over-stressed notches} \end{aligned}$$

where S_y is the yield point of the material limiting the level of the residual stresses, that is, the base metal yield in the case of weldments or the yield point of peened material in the case of shot peening.

The residual stresses on the surface of peened mild steel weldments were found to be 50-60% of S_u of the heat-affected-zone before peening as is commonly assumed for mild steels [6]. The peening induced residual stresses in the higher strength steels were found to follow the relationship [6]: $\sigma_r = -(0.21 S_u + 551)$ MPa. While one usually assumes that stress relieving reduces the residual stresses to zero, in fact, the residuals are reduced only to the value of the yield strength of the material at the stress relief temperature which is not necessarily zero.

2.4 Material Properties (Tasks 4 - 6)

Determining the fatigue crack initiation life requires measured or estimated values of many material properties. Surprisingly, the estimated fatigue crack initiation life and long life fatigue strength are rather insensitive to material properties, and small changes in properties usually do not cause large changes in the estimated results. In fact, a major role of yield (or ultimate) strength is limiting the maximum value of residual stress which can be sustained. The properties required in Tasks 8 and 10 are tabulated below:

Set-up Cycle Analysis (Task 8):

Young's Modulus	E
Yield Strength*	S_y
Ultimate Strength	S_u
Peterson's Material Constant*	a
Monotonic Stress-strain properties	K,n
Cyclic stress-strain properties	K',n'

Damage Analysis (Task 10):

Fatigue strength coefficient*	σ_f'
Fatigue strength exponent*	b
Stress relaxation exponent	k
Ultimate Strength	S_u

These properties can be measured using the tensile test (Task 4), cyclic stress-strain studies (Task 5), and cyclic stress relaxation tests (Task 6).

Since performing these tests is time consuming, expensive, and in some cases nearly impossible, it is useful to establish correlations of these required properties with ultimate strength or hardness of the notch-root material. Each of the material properties above denoted with an asterisk (*) can be correlated with ultimate strength which in turn is related to hardness. Thus, using the hardness of the notch-root material, it is possible to estimate the material properties needed in the analysis using the expressions below (MPa-mm units) (see also Figs. 4 and 5) [7]:

Yield strength of hot-rolled steel	$S_y \approx 5/9 S_u$
Yield strength of normalized steel	$S_y \approx 7/9 S_u - 138$
Yield strength of quenched and tempered steel	$S_y \approx 1.2 S_u - 345$
Peterson's material constant for steel	$a \approx 1.087 \times 10^5 S_u^{-2}$
Fatigue strength coefficient for steel	$\sigma_f' \approx 345 + S_u$
Fatigue strength exponent for steel	$b \approx -1/6 \log[2(1+345/S_u)]$

The monotonic stress-strain properties (K,n) are best estimated directly from tensile test data and the cyclic stress properties (K',n') are best estimated from cyclic test data; although the set-up cycle can often be performed using only the monotonic and elastic properties.

The cyclic stress relaxation exponent (k) depends both upon the material and the applied strain. A reasonable correlation, the relaxation exponent (k) has been found to be related to the notch-root plastic strain amplitude (ϵ_{pa}):

$$k \propto \epsilon_{pa} \quad (4)$$

The available data for the relaxation exponent are plotted in Fig. 6 [1,8].

Two other facts are worth noting. The elevation of hardness for peened mild steel has been found to be 1.2 times the original hardness for structural steels (see Fig. 7 [9]). Secondly, the hardness of grain coarsened heat-affected-zones of weldments has been found to vary systematically with base metal hardness; and for fusion welding processes typical of structural welding, the hardness of the grain coarsened heat-affected-zone is generally 1.5 times the hardness of the base metal (see Fig. 8). These two observations facilitate the estimation of fatigue life and strength for peened and welded components.

2.5 Estimating the Fatigue Notch Factor (Task 7)

In cases in which the elastic stress concentration factor (K_t) and the notch-root radius are known and defined, one can calculate the fatigue notch factor (K_f) using Peterson's equation (Eq. 2) and estimated or measured values of the material parameter (a). There have been many efforts to give physical significance to K_f [10], and a useful concept is that K_f represents the intensification of stress at the most distant region from the notch tip at which the initiation and early crack growth phenomena are the dominant fatigue mechanisms. Thus, K_f is generally less than K_t except for very large notch-root radii.

For many engineering notches, the notch-root radius is highly variable. Examples of such notches are weld toes or simple notches such as circular holes which have been exposed to corrosion. It is difficult to determine K_f for such notches because their notch-root radii are generally unknown, difficult to measure and highly variable. To cope with the variable nature of such notches, we have developed the concept of the "worst-case notch" in which a radius giving the highest possible value of fatigue notch factor is presumed to occur somewhere at the notch root. Our experience with the notch size effect for steels has led us to conclude that Peterson's equation correctly interrelates the fatigue notch and elastic stress concentration factors. The worst-case notch value of the fatigue notch factor, K_{fmax} , can be found by substituting Eq. 3 into Eq. 2 and differentiating with respect to r to find the value of notch-root radius for which the fatigue notch factor is maximum. Because the exponent in Eq. 3 is usually $1/2$, K_{fmax} occurs at notch-root radii numerically equal to Peterson's parameter a .

The concept of the worst-case notch and a graphical representation of the K_{fmax} concept are shown in Fig. 9. The value of K_{fmax} depends upon: the nature of the remote stresses (axial or bending) and the geometry of the joint through the constant (α), the ultimate strength of the material at the notch root (S_u) and the absolute size of the weldment through the dimension (t). The use of the worst-case notch concept leads to predictions that the fatigue strength of a notched component depends upon its size as well as its shape, material properties and manner of loading.

$$K_{fmax}^A = 1 + 0.0015\alpha_A S_u t^{1/2}$$

$$K_{fmax}^B = 1 + 0.0015\alpha_B S_u t^{1/2}$$
(5)

when both axial and bending stresses occur in an application K_{fmax} becomes a weighted average of K_{fmax}^A and K_{fmax}^B or K_{fmax}^{eff} :

$$K_{fmax}^{eff} = (1 - x) K_{fmax}^A + x K_{fmax}^B$$
(6)

where $x = S_a^B / S_a^T$; $S_a^T = S_a^A + S_a^B$. A and B represent the axial and bending loading conditions, respectively.

3. THE SET-UP CYCLE (TASK 8)

The notch-root stress amplitude (σ_a) and mean stress (σ_m) which prevail during the fatigue life of a notched component are established during the first few reversals of loading. If no notch-root yielding occurs during this time, one can skip over the set-up cycle analysis and assume elastic notch-root conditions. If notch-root yielding does occur during the first few applications of load, then a set-up cycle analysis should be performed, and failure to do so could lead to mistaken estimates of the notch-root conditions during fatigue.

The notch root stress ($\Delta\sigma$) can be related to the remote stresses (ΔS) through Neuber's rule:

$$\Delta\sigma\Delta\epsilon = (K_f\Delta S)^2/E$$
(7)

where $\Delta\sigma$ and $\Delta\epsilon$ are the notch root stresses and strain ranges, respectively and ΔS is the remote stress range which is within the elastic region. For the more complex but more general case involving both axial, bending and residual stresses, the notch-root stress-strain response for the first application of load (that is, the first reversal {0-1} as shown in Fig. 10) is limited by Neuber's rule modified for combined states of stress:

$$\Delta\sigma\Delta\epsilon = (K_f^A \Delta S_{0-1}^A + K_f^B \Delta S_{0-1}^B + \sigma_r)^2/E \quad (8)$$

where the superscript A is for the axial and the superscript B is for the bending loading conditions. The notch root stresses and strains at the end of the first reversal can be obtained by solving Eq. 8 above either analytically or graphically as shown in Fig. 10 using the monotonic stress-strain properties (K,n) and the power law relation:

$$\Delta\epsilon = \frac{\Delta\sigma}{E} + z \left(\frac{\Delta\sigma}{zK} \right)^{\frac{1}{n}} \quad (9)$$

where z equals 1 for the first reversal and equals 2 for subsequent reversals.

The notch-root stresses and strains at the end of the second {1-2} and subsequent reversals can be found in a similar manner using the cyclic stress-strain properties (K',n') and the expression below:

$$\Delta\sigma\Delta\epsilon = (K_f^A \Delta S_{1-2}^A + K_f^B \Delta S_{1-2}^B)^2/E \quad (10)$$

At the end of the first full cycle of the load history (2 or 3 reversals), one can determine the (stabilized) notch-root stress amplitude (σ_a) and mean stress (σ_m). It is assumed in this analysis that the material does not strain harden or soften and at the end of the first full cycle of the load history (2 or 3 reversals), one can determine the (stabilized) notch-root stress amplitude (σ_a) and mean stress (σ_m). It is further assumed that the stress amplitude and mean stress after the set-up cycle remain unchanged except for the possibility that the notch-root mean stress may relax with continued cycling.

Several interesting consequences of the set-up cycle analysis are shown in Figs. 10-12. In Fig. 11 [11] one can see that the role of residual stress depends greatly upon the amount of plasticity in the first cycle. Very ductile materials may wash-out any notch-root residual stress during the set-up cycle. Figures 10 and 12 show that the initial value of notch-root residual stress may be greatly altered and even be changed in sign from tension to compression or from compression to tension by the set-up cycle.

In the case of variable load histories, one customarily assumes that the history begins with the largest stress or strain event, and it is this series of reversals which is dealt with in the set-up cycle analysis.

4. THE DAMAGE ANALYSIS (TASK 10)

4.1 Predicting the Fatigue Behavior Under Constant Amplitude Loading With No Notch-Root Yielding or Mean-Stress Relaxation

Under the simplest conditions, the fatigue strength (S_a) of a notched component at given long lives can be estimated using the expression below:

$$\Delta S_a K_f = (\sigma_f' - K_f S_m - \sigma_r)(2N_I)^b \quad (11)$$

where S_a is the remote stress amplitude, σ_r is the notch-root residual stress and S_m is the applied mean stress or the global residual stress in the structure near the notch. A simple expression for the fatigue strength of notched members at long lives can be obtained from the expression above.

$$S_a = \left(\frac{\sigma_f' - \sigma_r}{K_f} \right) \left(\frac{(2N_I)^b}{1 + \frac{1+R}{1-R} (2N_I)^b} \right) \quad (12)$$

since $S_m = S_a(1+R/1-R)$. The above expression can be used only in the simplest case: at long lives (in quasi-elastic notch root conditions), when the K_f of the notch is known, when the residual stresses do not relax, when the loads are either purely axial or pure bending, and when the load history is constant amplitude.

Eq. 12 which is rewritten below to incorporate the concept of K_{fmax}^{eff} :

$$S_a^T = \frac{(\sigma_f' - \sigma_r)(2N_I)^b}{K_{fmax}^{eff} \left[1 + \frac{1+R}{1-R} (2N_I)^b \right]} \quad (13)$$

where

$$K_{fmax}^{eff} = (1-x)K_{fmax}^A + xK_{fmax}^B \quad (6)$$

$$x = S_a^D / S_a^T$$

A comparison of fatigue strength predictions made using Eq. 13 and experimental data for both as-welded and post-weld treated steel weldments [9] is given in Fig. 13. The fatigue strength S_a^T predicted by Eq. 13 can be plotted in a manner similar to K_{fmax} for a weldment of a given material and post-weld treatment. Since the fatigue strength coefficient (σ_f'), the fatigue strength exponent (b), the residual stress (σ_r), and K_{fmax} all depend upon or can be correlated with hardness or ultimate strength of the base metal, Eq. 13 can be expressed as a function of the ultimate strength and constants which depend upon ultimate strength and the type of post-weld treatment:

$$S_a^T = \frac{AS_u + B}{C(K_{fmax}^{eff} - 1) + 1} \cdot \frac{(2N_I)^b}{1 + \frac{1+R}{1-R} (2N_I)^b} \quad (14)$$

where:

S_u = tensile strength of base metal

$$b = -1/6 \log[2(1 + D/S_u)]$$

K_{fmax}^{eff} is calculated using the ultimate strength of base metal

(see Eq. 13)

A,B,C,D = coefficients given in Table 1 and below

$$AS_u + B = CS_u + 344 + \sigma_r$$

$$\begin{aligned} \sigma_r &= \pm S_y(BM) = 5/9 S_u && \text{Hot rolled} \\ &= 7/9 S_u - 138 && \text{Normalized} \\ &= 1.2 S_u - 345 && \text{Quenched and tempered} \end{aligned}$$

$$\sigma_r = 0 \quad \text{Stress relieved}$$

$C = 1$ Plain plate
 $= 1.5$ HAZ (stress relief might reduce this value)
 $= 1.5 \times 1.2 = 1.8$ Peened HAZ
 $D = 344/C$

TABLE 1

Coefficients of equation (14) for each post-weld treatment and base metal heat treatment

Post-weld treatment	Base metal heat-treatment	A	B	C	D
1. Plain plate	-	1	345	1.0	345
2. As-welded	Hot-rolled	0.94	345	1.5	230
	Normalized	0.72	483	1.5	230
	Q&T	0.30	690	1.5	230
3. Stress-relief	-	1.50	345	1.5	230
4. Over-stressed	Hot-rolled	2.06	345	1.5	230
	Normalized	2.28	207	1.5	230
	Q&T	2.70	0	1.5	230
5. Shot-peening	S_u (HAZ)	2.12	896	1.8	191
	<862 Mpa				
	S_u (HAZ)	2.12	896	1.8	191
	>862 Mpa				

Units: t (mm); S_u (MPa).

Figure 14 gives an example of the graphical determination of the fatigue strength of weldments based upon Eq. 14 for as-welded ASTM A36 steel. Comparison of the conditions described by lines A→A''' and B→B''' show that welds with more favorable geometries (A→A''') may have lower fatigue strengths than weldments having worse geometries but smaller thicknesses, having smaller flank angles, and having a smaller R ratio. Comparison of

line B→B''' with line C→C''' shows that weldments subjected to bending (C→C''') give higher fatigue lives than smaller weldments subjected to more nearly axial loading conditions (B→B''').

Figures 15 and 16 give similar graphical aids for ASTM A36 in the post-weld treated (stress-relieved and shot-peened) conditions, respectively. These design aids are based entirely upon Eq. 14 above. Nomographs for other steels and other notch geometries can be constructed in a similar way.

The accuracy of predictions based on Eq. 14 requires further study, but comparison of predictions made using Eq. 14 and available test data is given in Fig. 13. If one discounts the data for stress-relieved and hammer-peened weldments (treatments which may not be as effective as hoped), then Eq. 14 would seem to predict the fatigue strength of steel weldments with an accuracy of roughly 25%.

4.2 Predicting the Fatigue Behavior Under Constant Amplitude Loading With Notch-Root Yielding and No Mean-Stress Relaxation

When the notch-root conditions are not quasi-elastic and substantial plastic deformation occurs during the set-up cycle (Task 8,) the simple expressions developed in the preceding section cannot be used. When there is notch-root yielding during the set-up cycle but no mean-stress relaxation during subsequent cycling, the notch-root stress amplitude (σ_a) and mean stress (σ_m) determined in the set-up cycle can be substituted into Eq. 1 to estimate (the long life) fatigue strength or fatigue crack initiation life (N_I).

4.3 Predicting the Fatigue Crack Initiation Life Under Constant Amplitude Loading With Notch-Root Yielding and Mean-Stress Relaxation

In general, there are several possible outcomes which may result from the notch-root residual stresses which exist prior to the set-up cycle: There may be substantial notch-root mean stresses after the set-up cycle or there may be none; subsequent to the set-up cycle, any non-zero notch-root mean stress may persist for the duration of the fatigue life or it may relax. The outcome in which notch-root mean stresses exist after the set-up cycle but relax during fatigue cycling requires a special analysis.

If the mean stress established during the set-up cycle relaxes during cycling, the current value of mean stress ($\sigma_{m,2N}$) can be predicted using a power function (see also Fig. 17):

$$\sigma_{m,2N} = \sigma_{m,i} (2N-1)^k \quad (15)$$

where k is the relaxation exponent determined in Task 9 using the material properties describing stress relaxation (Task 6) and the notch-root stresses and strains determined in the set-up cycle analysis (Task 8); $\sigma_{m,i}$ is the notch-root mean stress after the set-up cycle; and $2N$ is the elapsed reversals. Larger plastic strain amplitudes and higher mean stresses cause a more rapid relaxation of notch-root mean stress. Using the above expression for the current value of notch-root mean stress and the Basquin equation (Eq. 1), one can solve for the fatigue crack initiation life ($2N_I$) as the upper limit of integration of the equation below:

$$\int_1^{2N_I} \{(\sigma_f'/\sigma_a)(1 - (\sigma_{m,i}/\sigma_f')(2N_i)^k)\}^{-1/b} dN_i = 1 \quad (16)$$

Typical behavior of Eq. 16 above is shown in Fig. 18.

4.4 Predicting the Fatigue Crack Initiation Life Under Variable Load Histories Without Mean Stress Relaxation

For variable amplitude load histories the linear cumulative damage rule is used to sum up the fatigue damage rate (D_i) of each closed hysteresis loop in one block of the load history ignoring the possibility of notch root mean stress relaxation [12]:

$$D_{\text{block}} = \sum D_i = \sum \left[\frac{\sigma_f' - \sigma_m}{\Delta\sigma/2} \right]_i^{-1/b} \quad (17)$$

then N_I is the reciprocal of D_{block}

$$N_I = 1/D_{\text{block}}$$

Although many cycle counting methods have been proposed in the past years, the 'vector method' concept developed by Dowling and Socie [13] is considered to be the most effective and easier to program for a digital computer. For a notched member without bending stresses and residual stresses, the load history is rearranged in such a manner that the largest value of $(K_{fmax}^A S_i^A + K_{fmax}^B S_{i+\sigma_r}^B)$ as the first and last values while performing the cycle counting.

REFERENCES

1. Lawrence F.V., Jr., Mattos R.J., Higashida Y. and Burk J.D. (1978) Estimation of fatigue initiation life of weld. ASTM STP 684, 134-158.
2. Lawrence F.V., Jr., Ho N.-J. and Mazumdar P.K. (1980) Predicting the fatigue resistance of welds. FCP Report No. 36, University of Illinois at Urbana-Champaign.
3. Yung J.-Y. and Lawrence F.V., Jr. (1985) Fatigue of weldments under combined bending and torsion. Spring conference on experimental mechanics, Society for Experimental Mechanics, 646-648.
4. Peterson R.E. (1974) Stress concentration factors. John Wiley & Sons, Inc.
5. Yung J.-Y. and Lawrence F.V., Jr. (1985) Analytical and graphical aids for the fatigue design of weldments. Accepted for publication in Fatigue and Fracture of Engineering Materials and Structures.
6. Cichlar D. (1980) Private Communication, Metal Improvement Company, Chicago, Illinois.
7. McMahon J.C. and Lawrence F.V., Jr. (1984) Predicting fatigue properties through hardness measurements. FCP Report No. 105, University of Illinois at Urbana-Champaign.
8. Prine D.W., Malin V.D., Yung J.-Y., McMahon J. and Lawrence F.V., Jr. (1982) Improved fabrication and inspection of welded connections in bridge structures. U.S. Department of Transportation, Report No. FHWA/RD-83/006.
9. Chang, S.T. and Lawrence, F.V., Jr. (1983). Improvement of weld fatigue resistance. FCP Report No. 46, University of Illinois at Urbana-Champaign.
10. Chen, W.-C. and Lawrence, F.V., Jr. (1979). A model for joining the fatigue crack initiation and propagation analysis. FCP Report No. 32, University of Illinois at Urbana-Champaign.
11. Burk J.D. and Lawrence, F.V., Jr. (1978) Effect of residual stresses on weld fatigue life. Ph.D. Thesis, University of Illinois at Urbana-Champaign.
12. Ho N.-J. and Lawrence F.V., Jr. (1984) Constant amplitude and variable load history fatigue test results and predictions for cruciform and lap welds. Theoretical and Applied Fracture Mechanics 1, 3-21.
13. Dowling S.D. and Socie D.F. (1982) Simple Rainflow Counting Algorithms, International Journal of Fatigue 4, 31-40.
14. Paris P.C. and Erdogan F. (1963) A critical analysis of crack propagation law. Journal of Basic Engineering ASME Transaction Ser. D 85, 528-534.

15. Elber W. (1974) Fracture toughness testing and slow stable cracking. ASTM STP 559, 45-58.
16. Maddox S.J. (1975) An analysis of fatigue cracks in fillet welded joints. International Journal of Fracture 11, 221-243.
17. Tada h. and Paris P.C. (1983) The stress intensity factor for a crack perpendicular to the welding bead. International Journal of Fracture 21, 279-284.
18. Al-Hassani S.T.S. (1982) The shot peening of metals - mechanics and structures. SAE Report No. 821452.
19. Smith I.F.C. and Smith R.A. (1983) Fatigue crack growth in a fillet welded joint. Engineering Fracture Mechanics 18, 861-869.
20. Nelson D.V. and Socie D.F. (1982) Crack initiation and propagation approaches to fatigue analysis. ASTM STP 761, 110-132.
21. Throop, J.F. (1983) Fracture mechanics analysis of the effects of residual stress on fatigue life. Journal of testing and Evaluation 11, 75-78.
22. Elber W. (1974) Fracture toughness testing and slow stable cracking. ASTM STP 559, 45-58.
23. Socie, D.F. (1977) Estimating fatigue crack initiation and propagation lives in notched plates under variable loading history. TAM Report No. 417, University of Illinois at Urbana-Champaign.

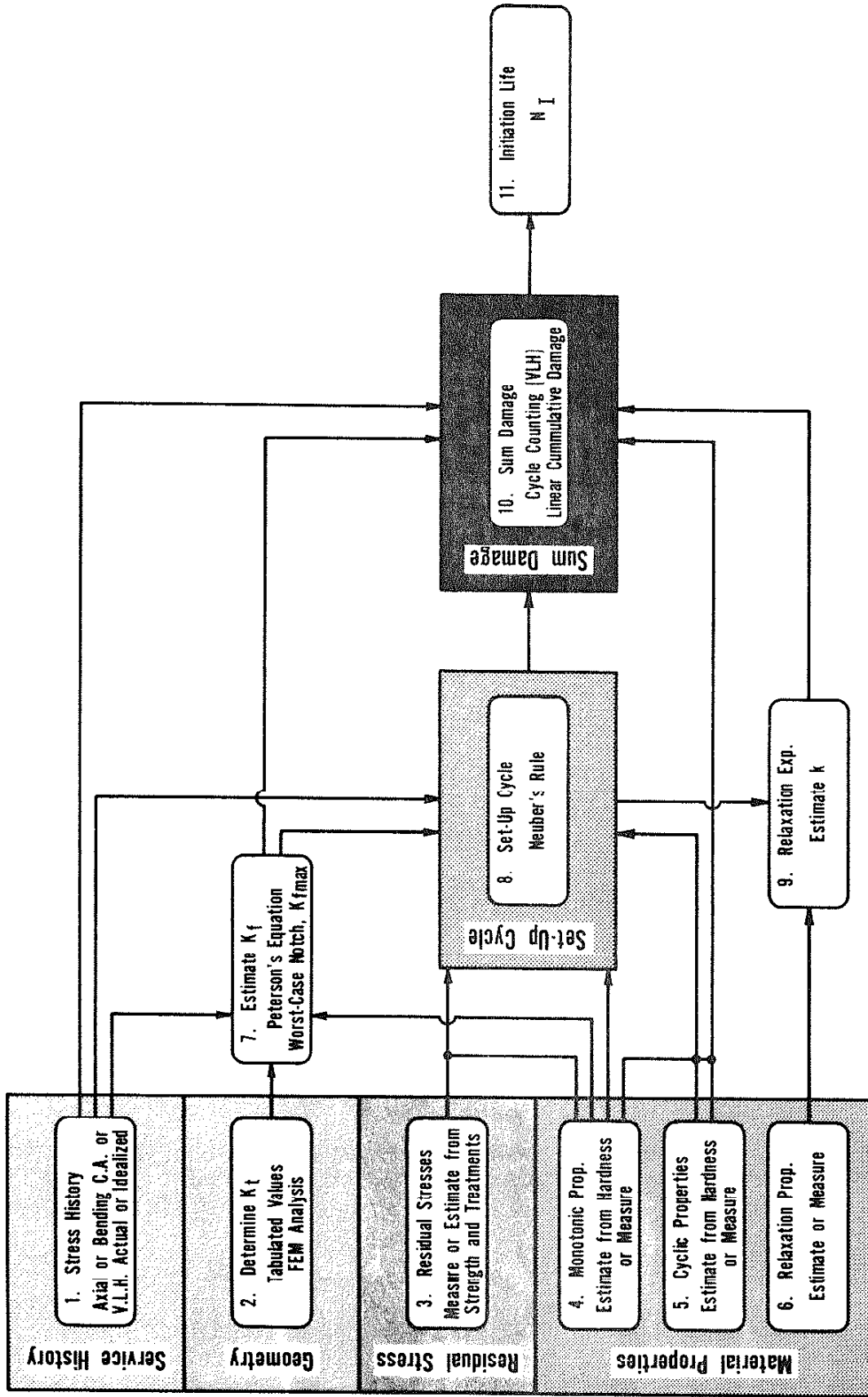


Fig. 1 Schematic diagram for the fatigue crack initiation life estimation procedure.

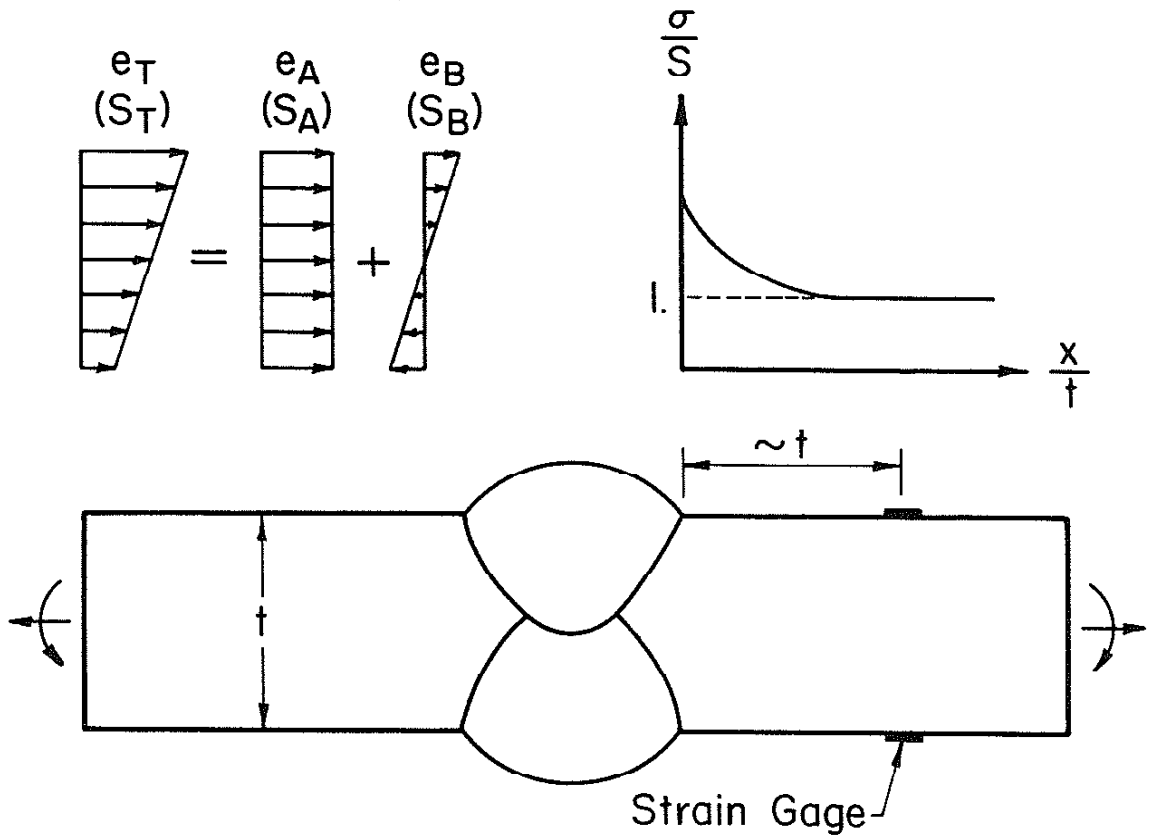


Fig. 2 The location of strain gages relative to the notch and the separation of remote axial and bending strains (stresses).

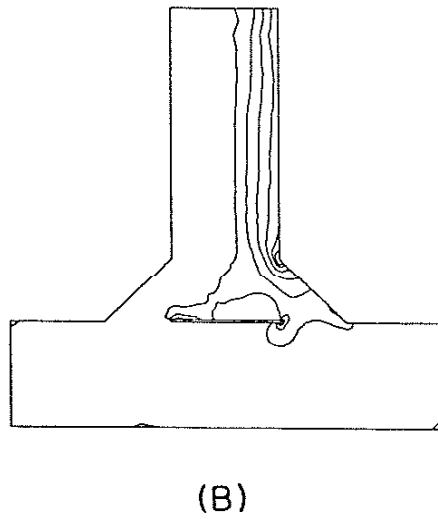
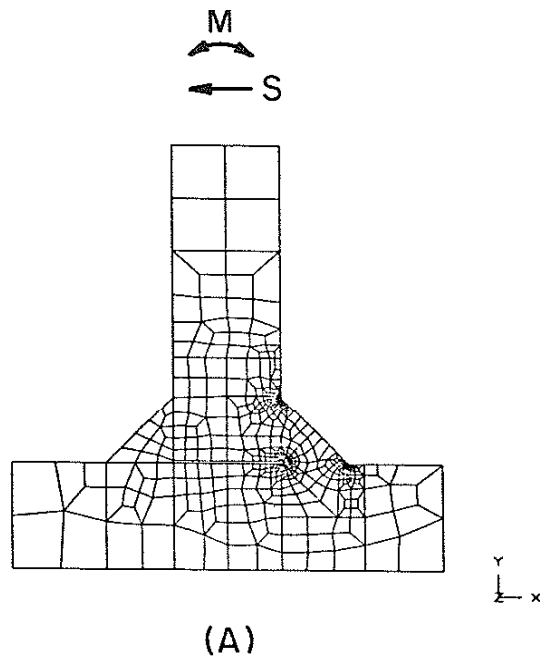


Fig. 3 (a) Finite element mesh for T joints subjected to bending and shear; (b) contours of tensile maximum principal stresses resulting from (a).

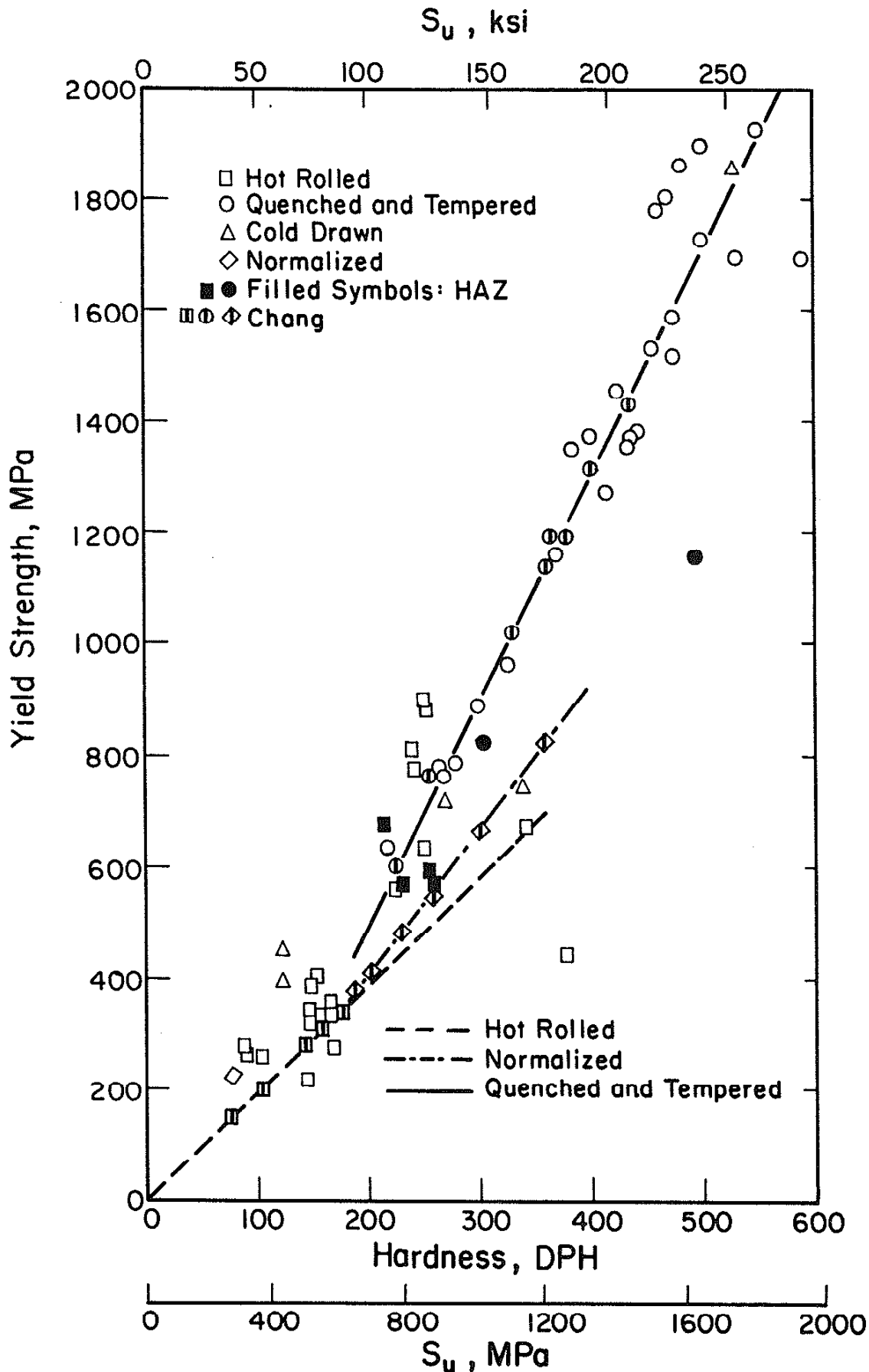


Fig. 4 Yield strength as a function of ultimate strength and hardness [7].

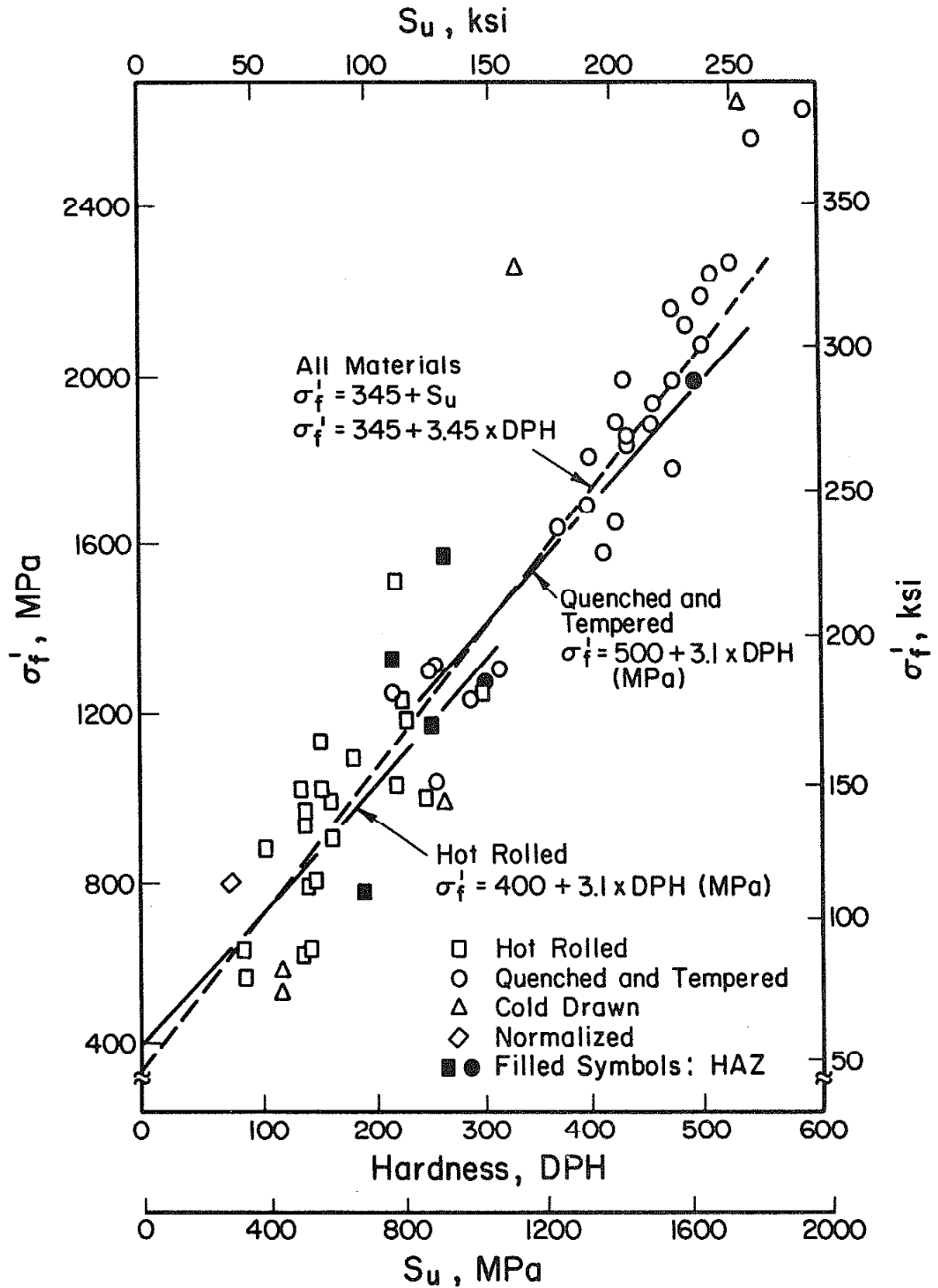


Fig. 5 Fatigue strength coefficient as a function of ultimate strength and hardness [7].

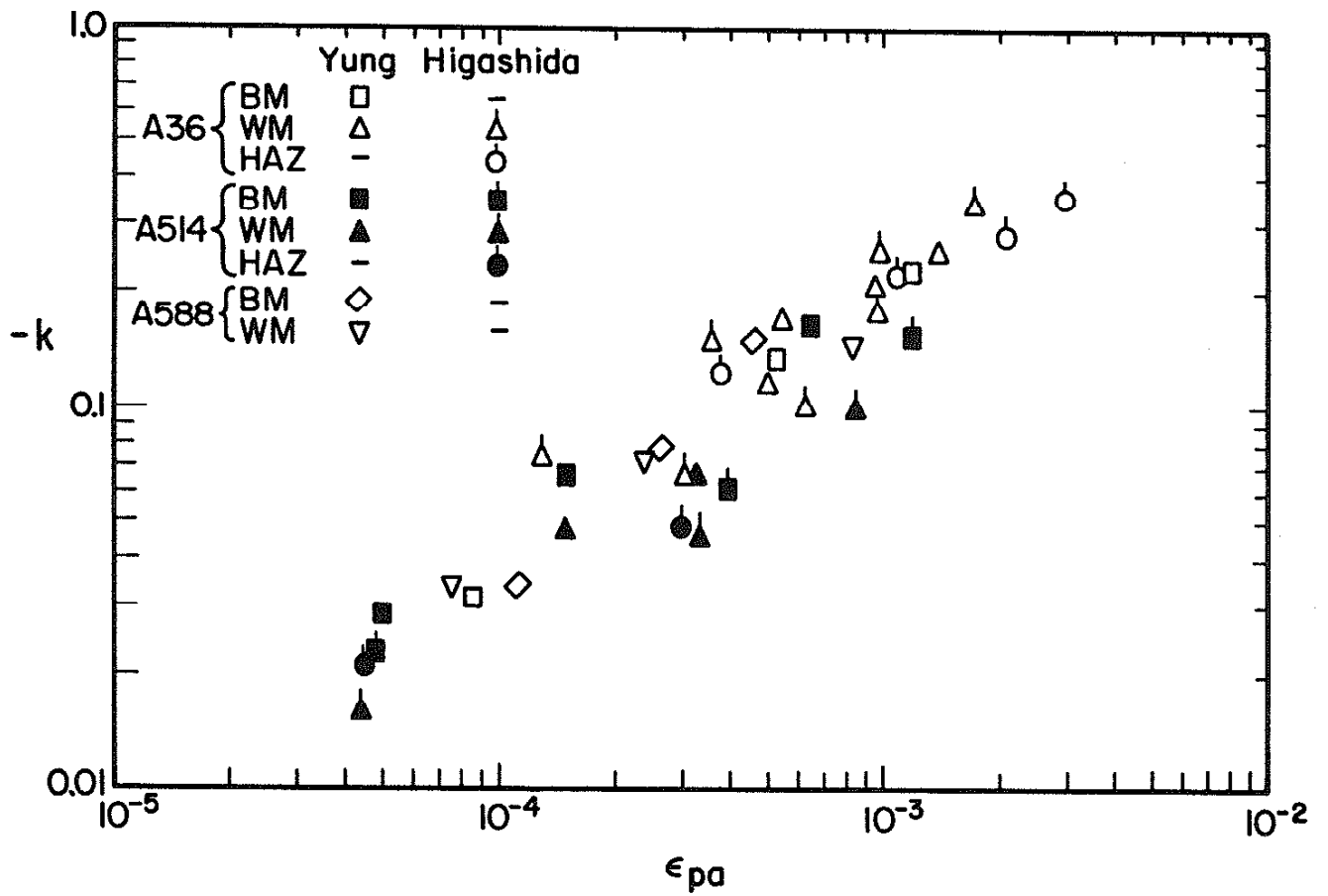


Fig. 6 Relaxation exponent as a function of plastic strain amplitude [1,8].

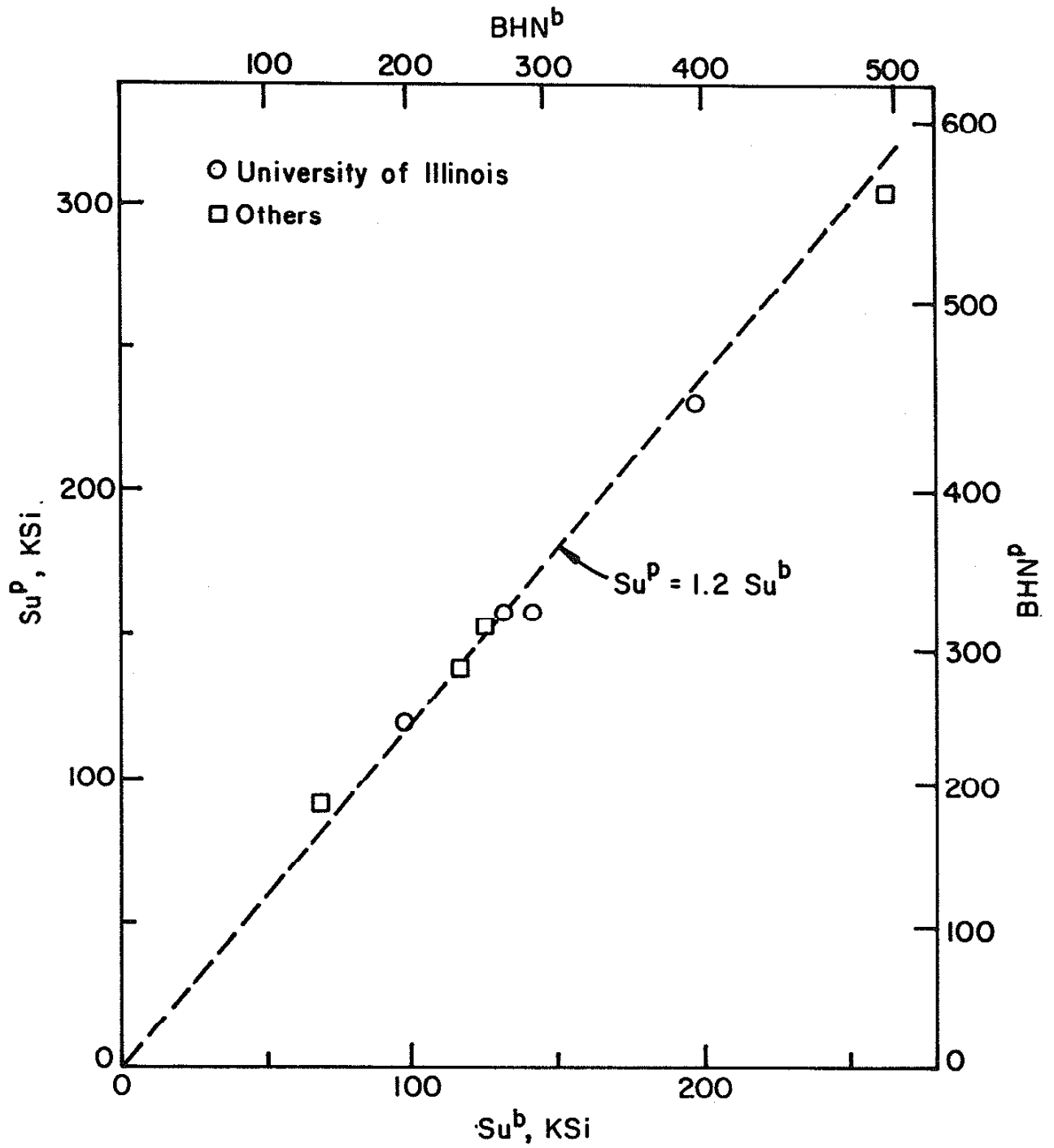


Fig. 7 Peened material hardness as a function of base metal hardness [9].

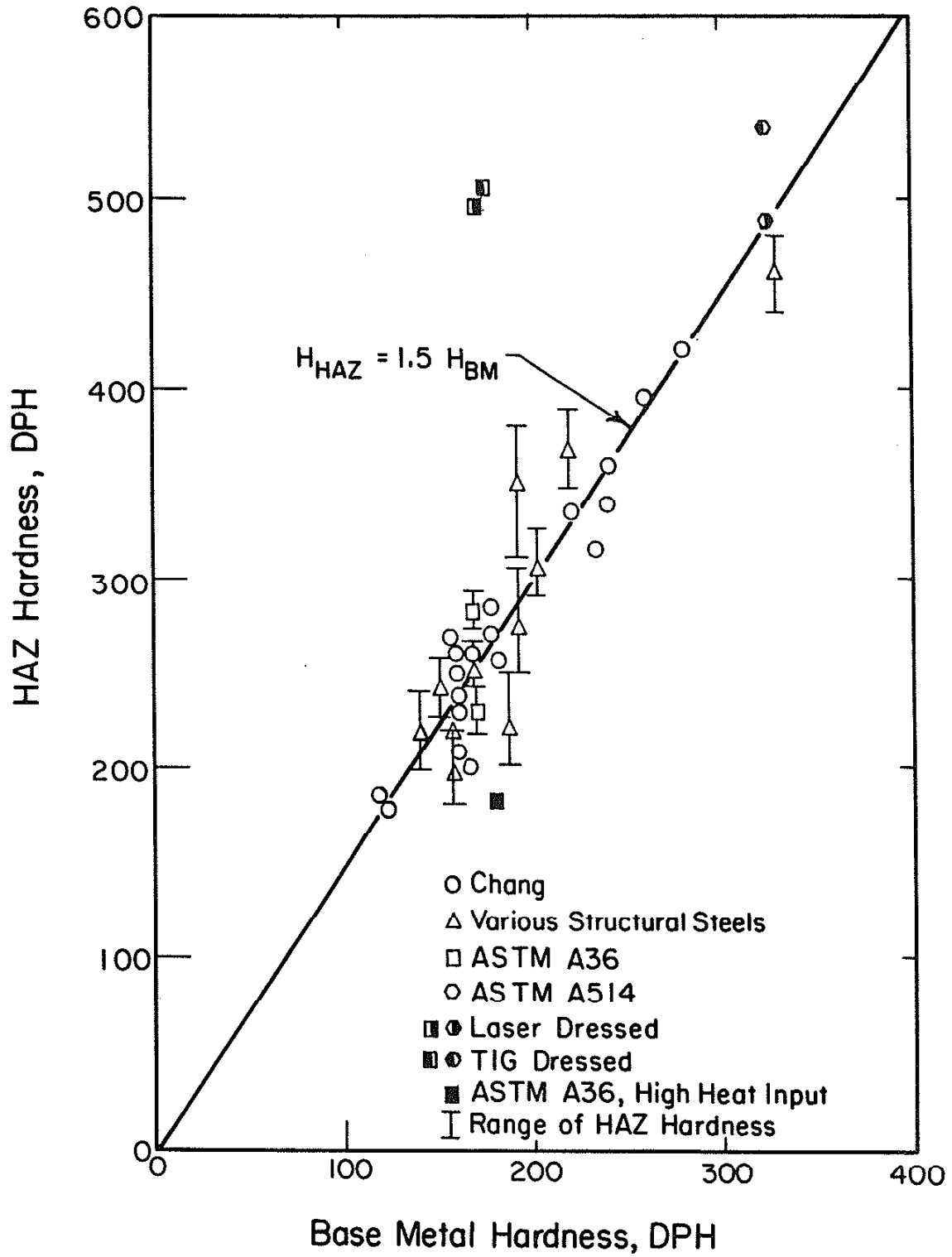


Fig. 8 Heat-affected-zone hardness as a function of base metal hardness [7].

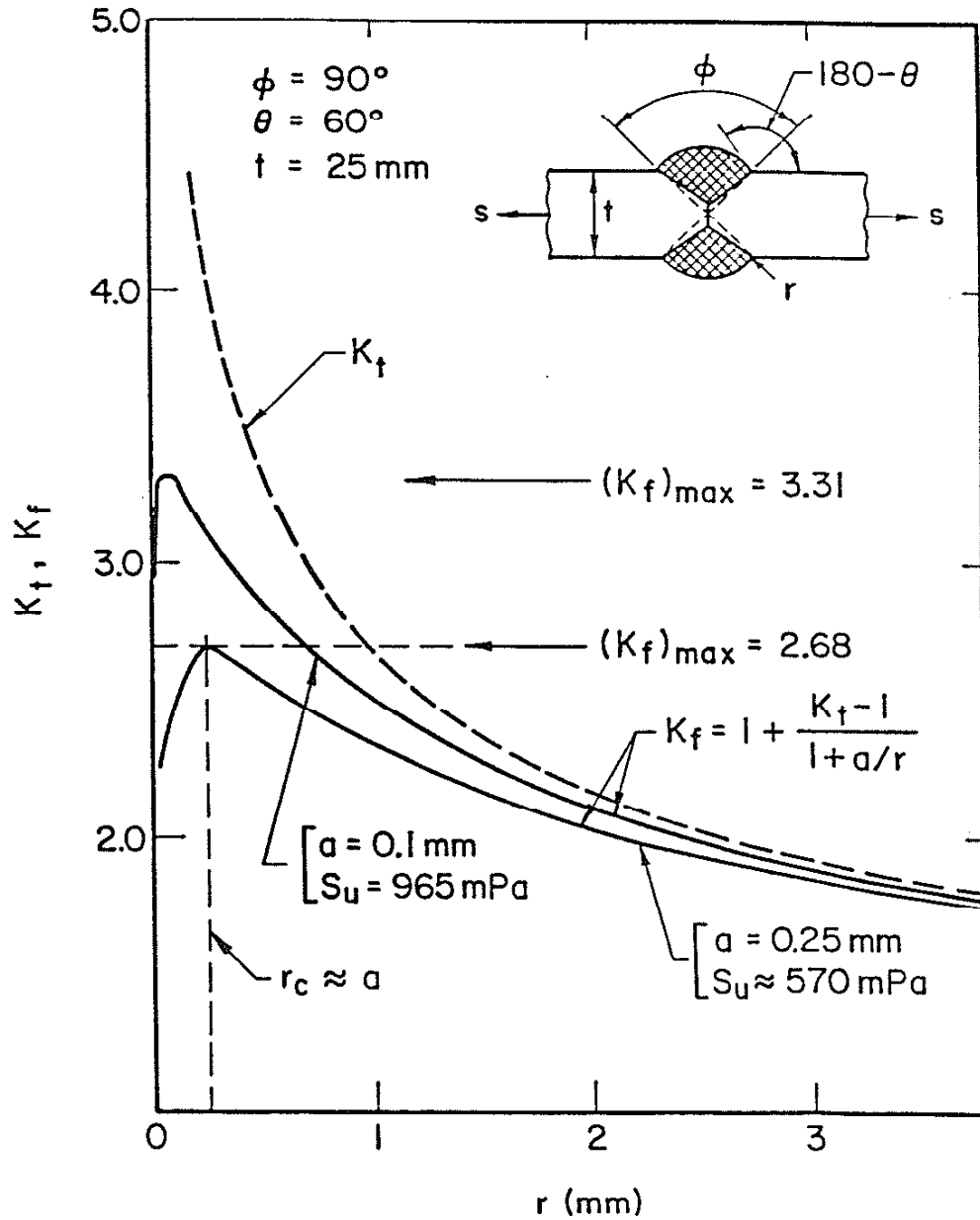


Fig. 9 Elastic stress concentration factor (K_t) and fatigue notch factor (K_f) as a function of toe root radius. $K_{f_{max}}$ is the "worst case" value of K_f for a given material and geometry.

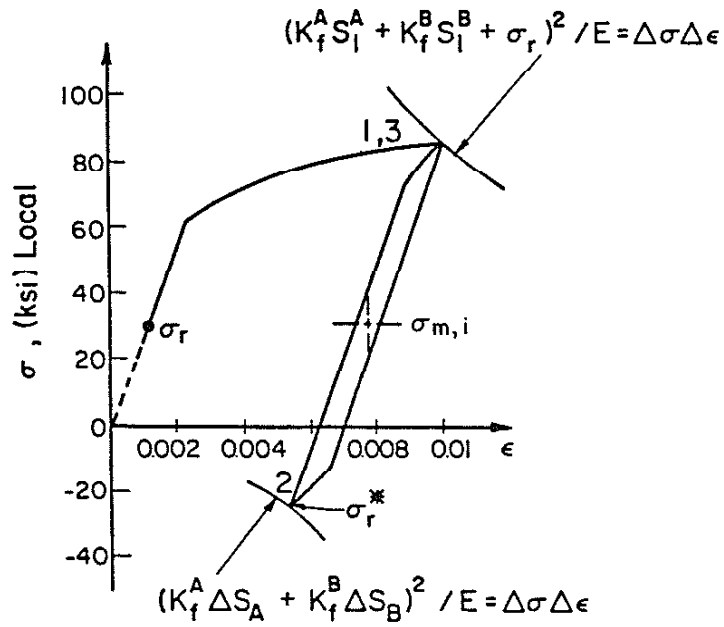
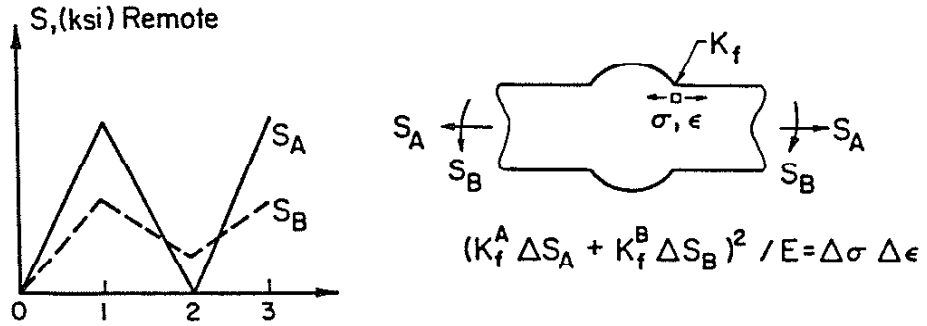


Fig. 10 Set-up cycle analysis for the weld toe with tensile residual stresses. Note the change of the sign of the notch-root residual stresses after the second reversal of load.

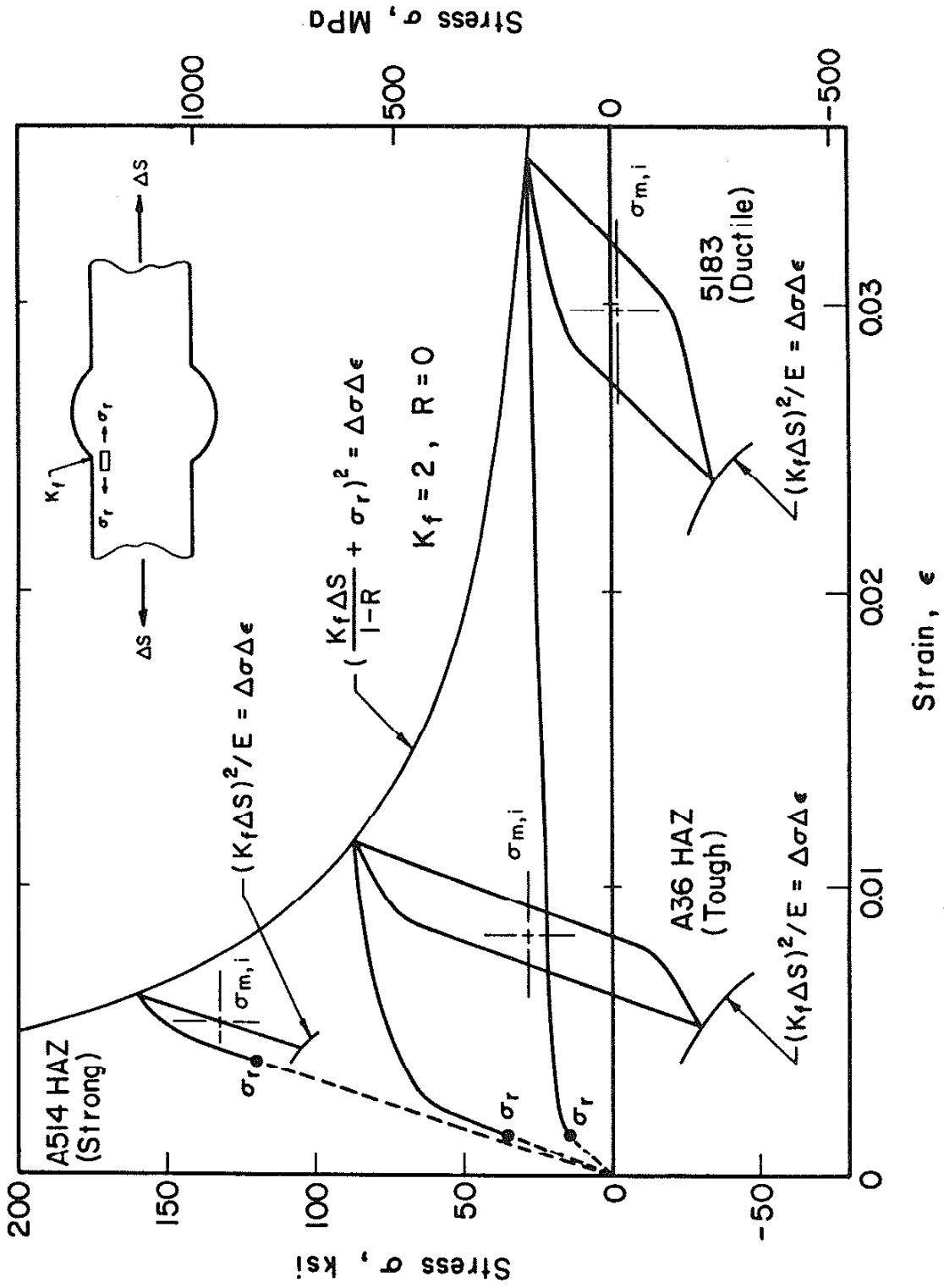


Fig. 11 Set-up cycle for ASTM A514 HAZ (strong), A36 HAZ (tough) steels, and aluminum alloy 5183 MM (ductile) materials [11]. The set-up cycle may eliminate notch-root residual stresses in ductile materials.

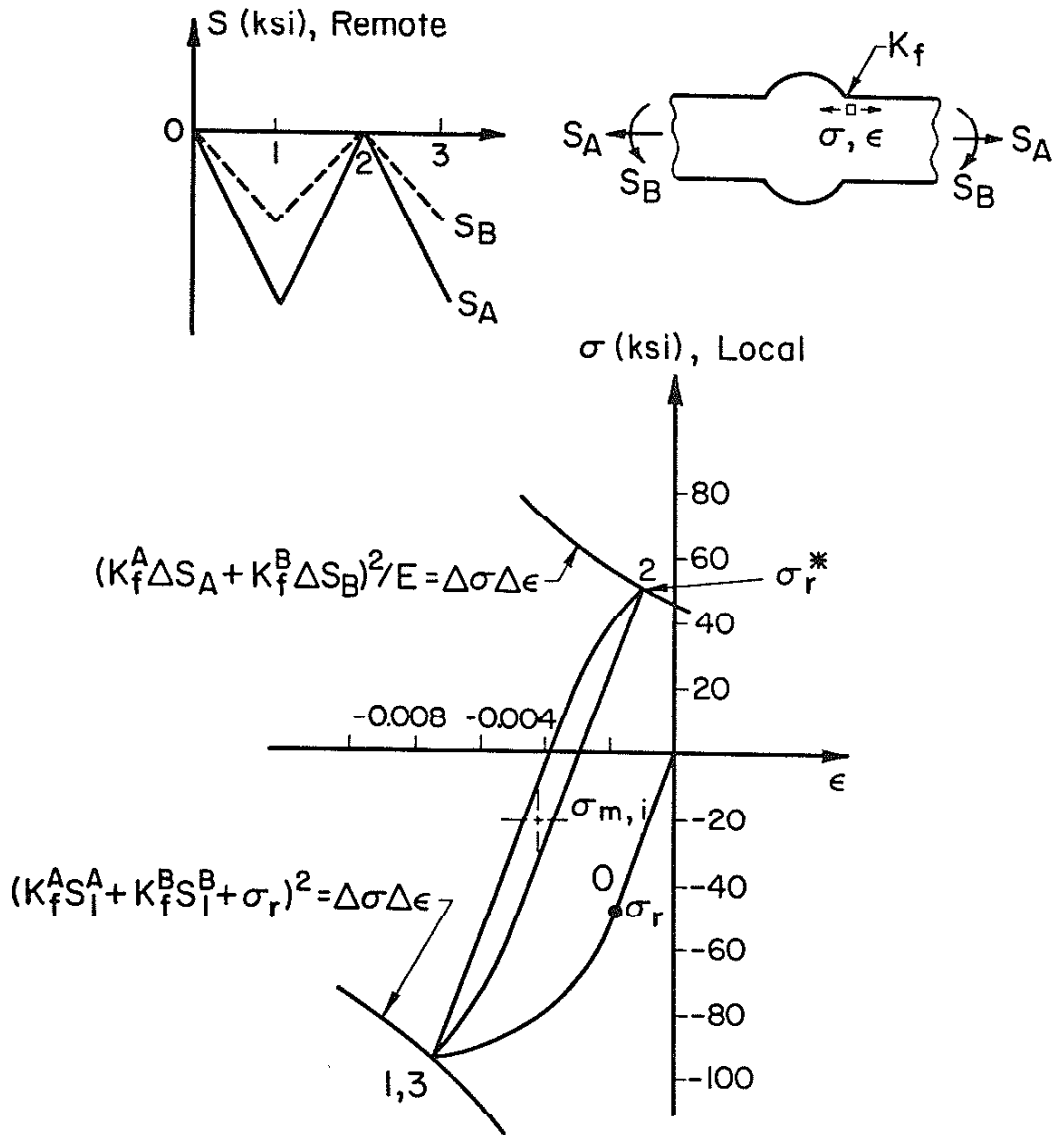


Fig. 12 Reversal of sign of residual stresses after set-up cycle. An example of compressive loadings and compressive residual stresses

ASTM-A36, AS-WELDED

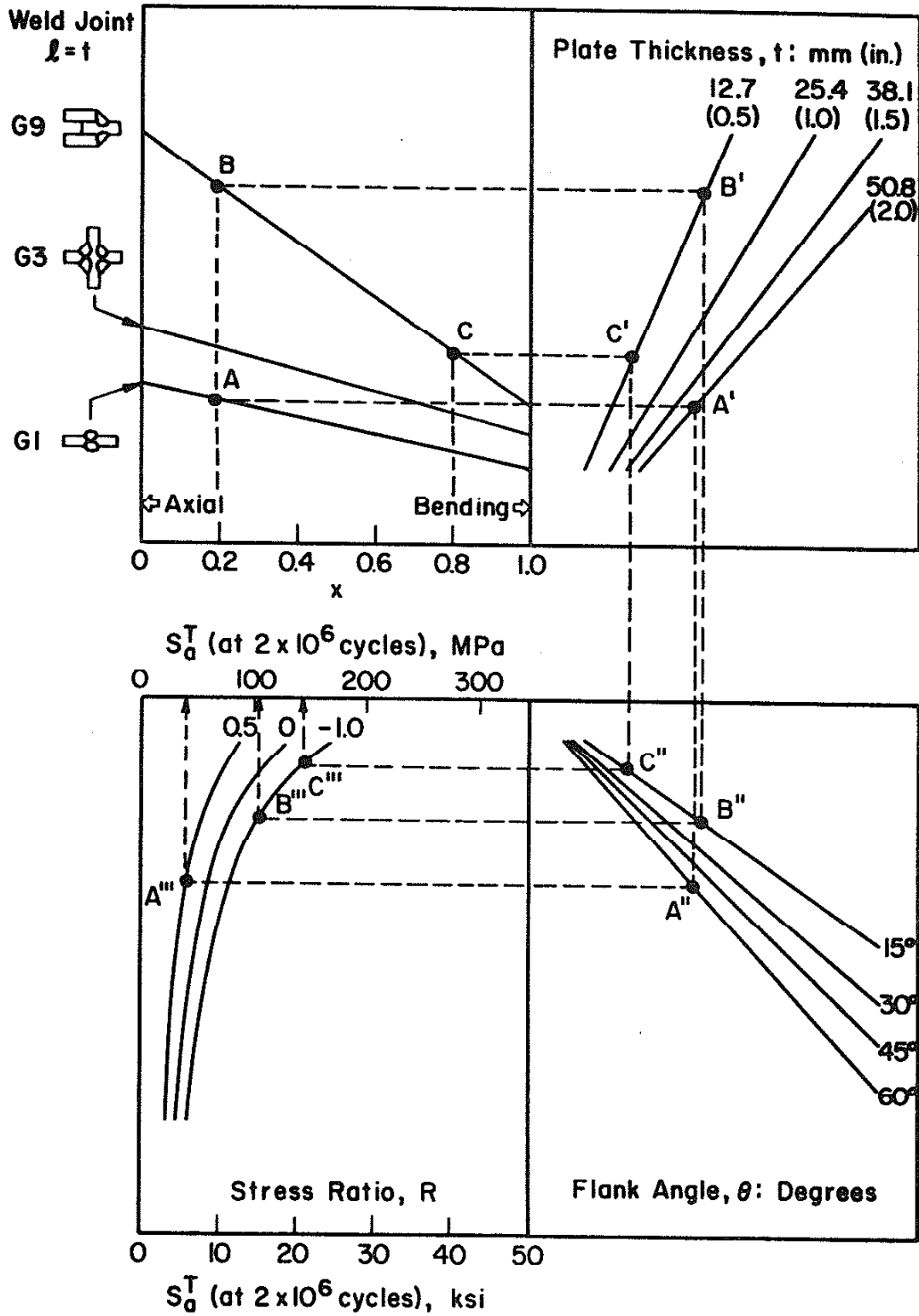


Fig. 14 Use of the proposed nomograph for the fatigue design of as-welded ASTM A36 steel weldments [5].

ASTM-A36, STRESS-RELIEVED

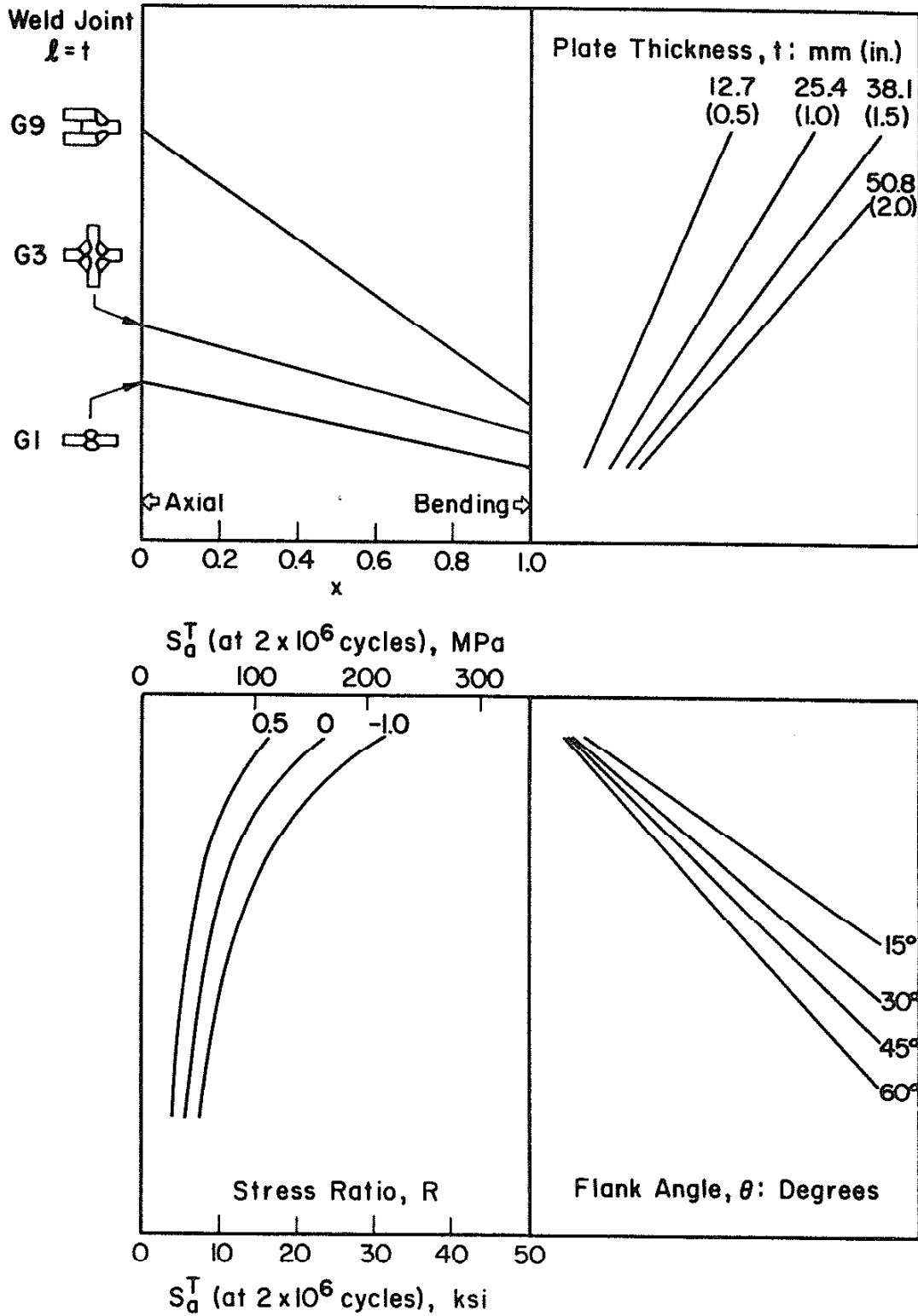


Fig. 15 Nomograph for the fatigue design of stress-relieved ASTM A36 weldments [5].

ASTM-A36, SHOT-PEENED

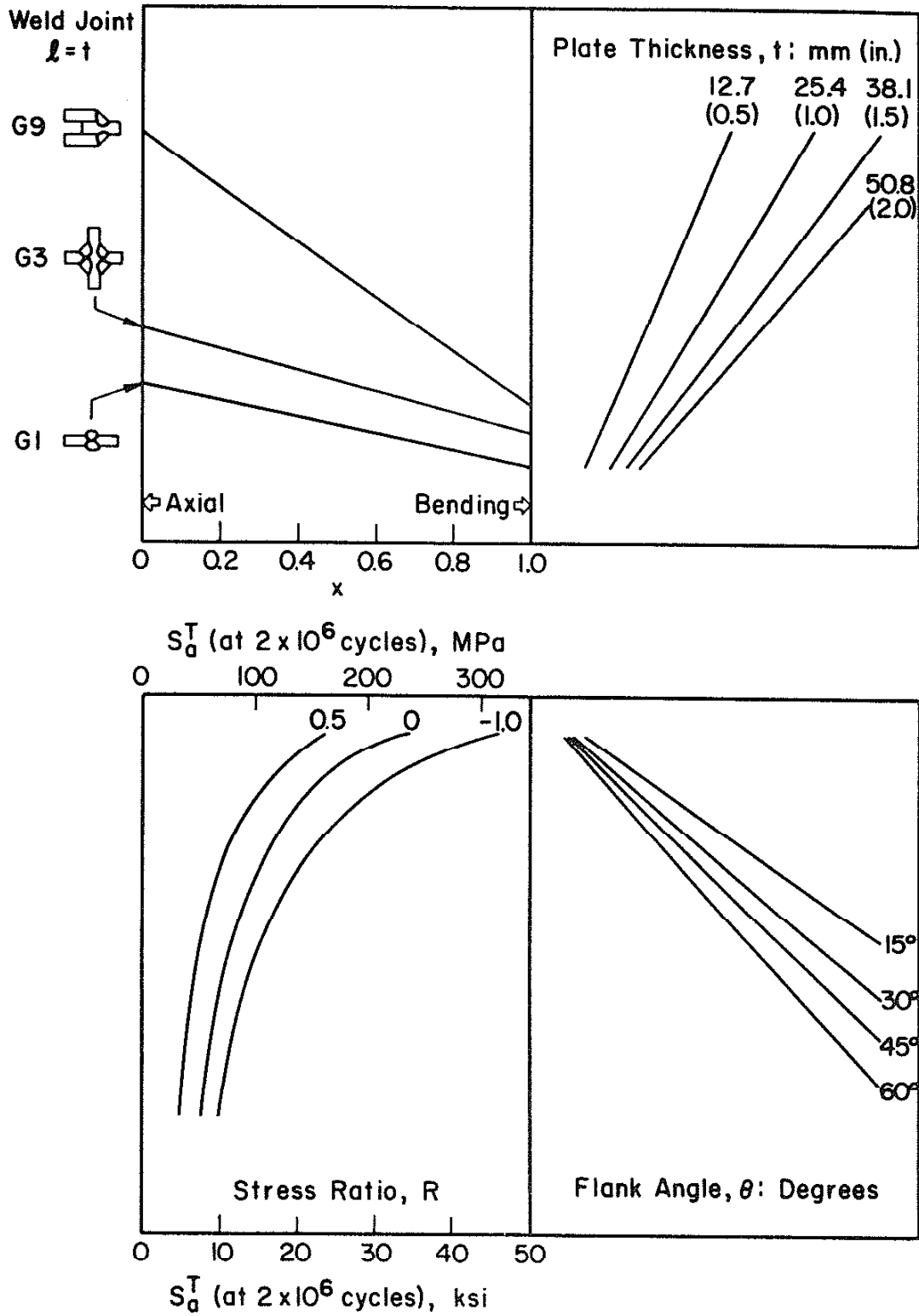


Fig. 16 Nomograph for the fatigue design of shot-peened ASTM A36 weldments [5].

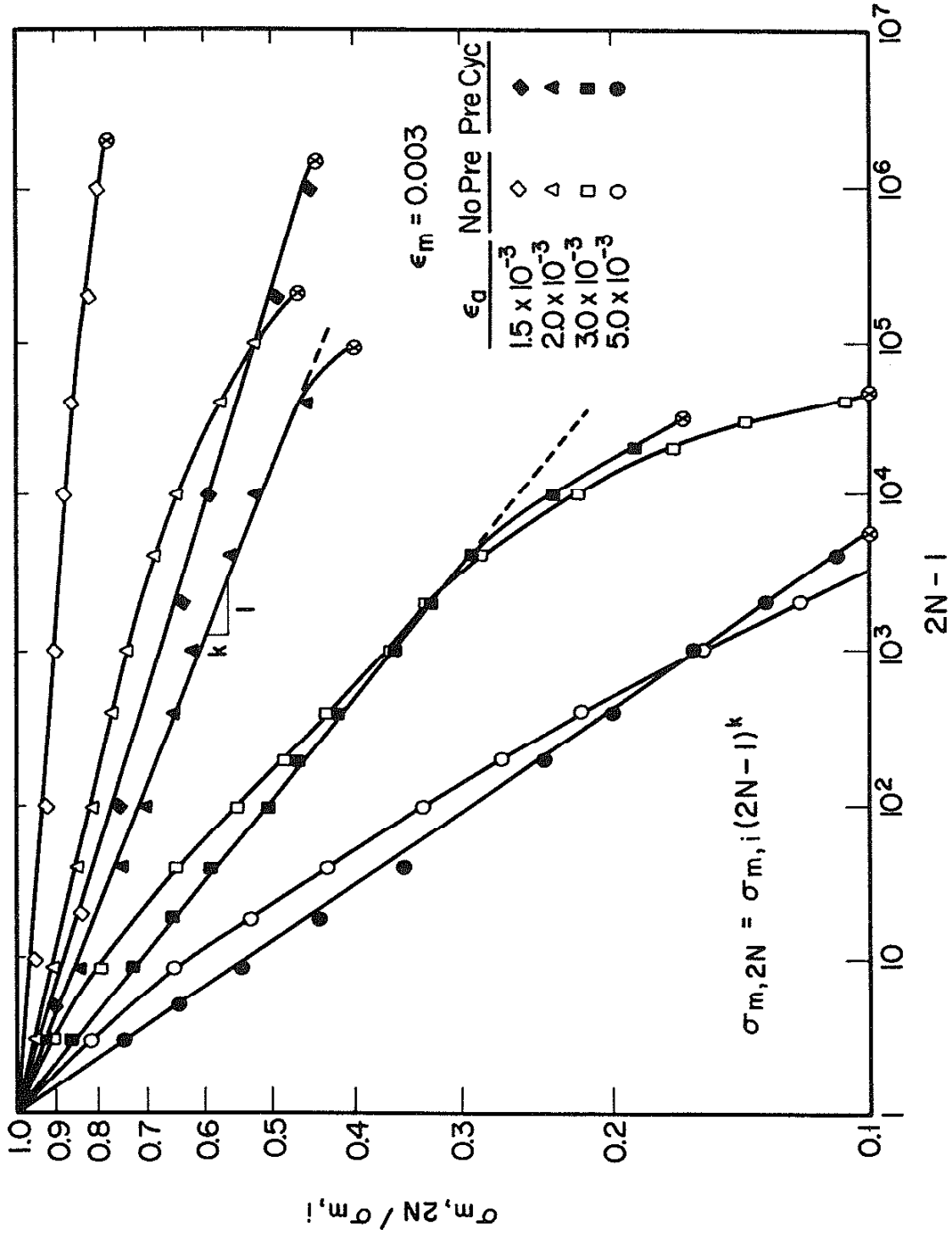


Fig. 17 Mean stress relaxation behavior as a function of cycles [11].

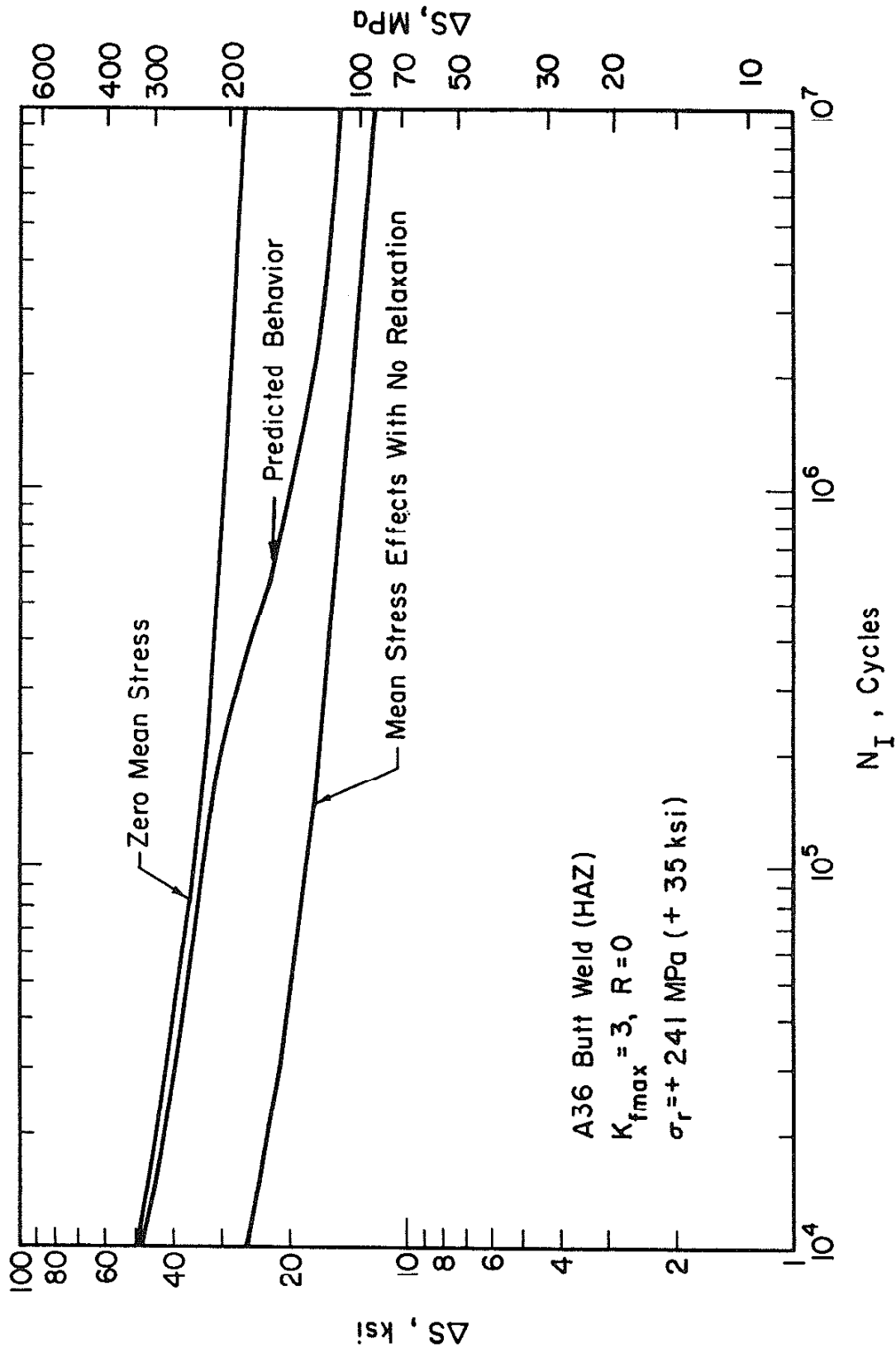


Fig. 18 Mean stress relaxation influence on the fatigue crack initiation life [11].

APPENDIX

ESTIMATING THE FATIGUE LIFE DEVOTED TO CRACK PROPAGATION (N_p)

The fatigue crack propagation life N_p for constant amplitude loading can be computed by integrating Paris' equation [14] from the initial crack length a_i to the final crack length a_f :

$$da/dN = C (\Delta K)^n \quad (A-1)$$

$$N_p = \int_{a_i}^{a_f} da / [C(\Delta K)^n] \quad (A-2)$$

where C and n are material constants, ΔK is the stress intensity factor range:

$$\Delta K = YS(\pi a)^{1/2} \quad (A-3)$$

where Y is the geometry factor.

Mean stress effect on crack propagation rate can be accounted for by substituting effective stress intensity factor range ΔK_{eff} [15] into Eq. A-1. For a given shape of weld, Y can be expressed conveniently by superposition of several geometry effects [16]:

$$Y = M_s M_t M_k / \phi_0 \quad (A-4)$$

in which M_s accounts for the effect of free front surface; M_t for the finite plate width w ; ϕ_0 for the crack shape; M_k for nonuniform stress gradient due to the stress concentration of weld discontinuity.

When a weld is subjected to combined loading of axial, induced bending and residual stress, the total stress intensity factor range ΔK_T can be obtained by a superposition method:

$$\Delta K_T = \Delta K_A + \Delta K_B + K_r \quad (A-5)$$

$$K_r = F_{\sigma_r} (\pi a)^{1/2} \quad (A-6)$$

where ΔK_A and ΔK_B are the stress intensity factors for tension and bending respectively, and K_r is the stress intensity factor due to residual stress and F is a function of residual stress distribution. When a crack is subjected to a distributed residual stress $\sigma_r(x)$, the stress intensity factor K_r is calculated by the integral:

$$K_r = \frac{2\sqrt{a}}{\pi} \int_0^a \frac{\sigma_r(x)}{(a^2 - x^2)^{1/2}} dx \quad (A-7)$$

Tada and Paris [17] derived the stress intensity factor for a crack perpendicular to a weld bead using Eq. A-7. The stress intensity factor caused by the residual stresses was expressed in a simple form shown in Fig. A1. It has been shown [19] that compressive residual stress has an influence on the fatigue crack propagation behaviour in hammer-peened welds. The ability of notch compressive residual stresses to retard fatigue crack growth depends on the distribution in depth of both the residual stresses and the local stresses, and the relaxation of the residual stresses in depth [20]. Figure A-2 shows the typical residual stress distribution for shot-peened specimens, and two hypothetical notch residual stress fields and their corresponding stress intensity factors [21,22]. Calculation of N_p is carried out by substituting ΔK_T into Eq. A-1.

The fatigue crack propagation life N_p for a weld under variable amplitude loading can be estimated using a method developed by Socie [23] and modified by Ho [9]. The crack growth rate per block $\Delta a/\Delta B$, is calculated by considering the crack length as being fixed at the initial crack size and summing the incremental crack extension for each cycle:

$$\Delta a/\Delta B = \sum \Delta a_i \quad (A-8)$$

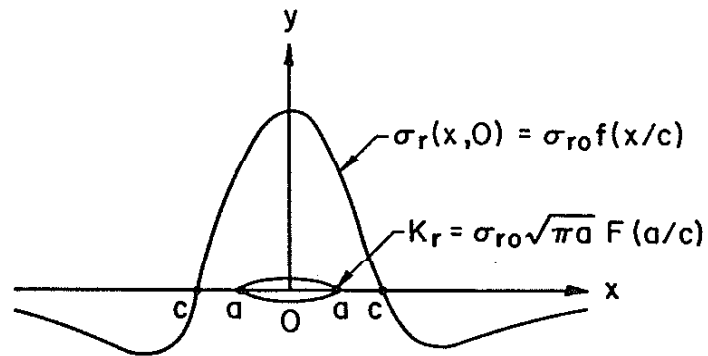
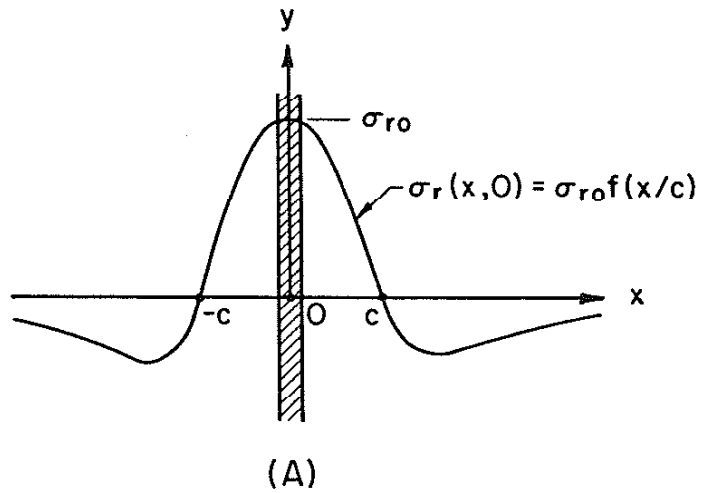
Combining Eqs. A-1, A-5, A-6, Eq. A-8 becomes

$$\Delta a/\Delta B = C (\pi a)^{n/2} \left[(Y_A \Delta S_A + Y_B \Delta S_B + F \sigma_r)^n \right] \quad (A-9)$$

Then, the crack propagation life N_p (in blocks) is

$$N_P = \int_{a_i}^{a_f} (\Delta B / \Delta a) da$$

(A-10)



$$F(a/c) = \left\{ \frac{[1 + (a/c)^4]^{1/2} - (a/c)^2}{1 + (a/c)^4} \right\}^{1/2}$$

Fig. A1 (a) Longitudinal residual stress field due to welding (hatched area: weld metal); (b) Crack in residual stress field [17].

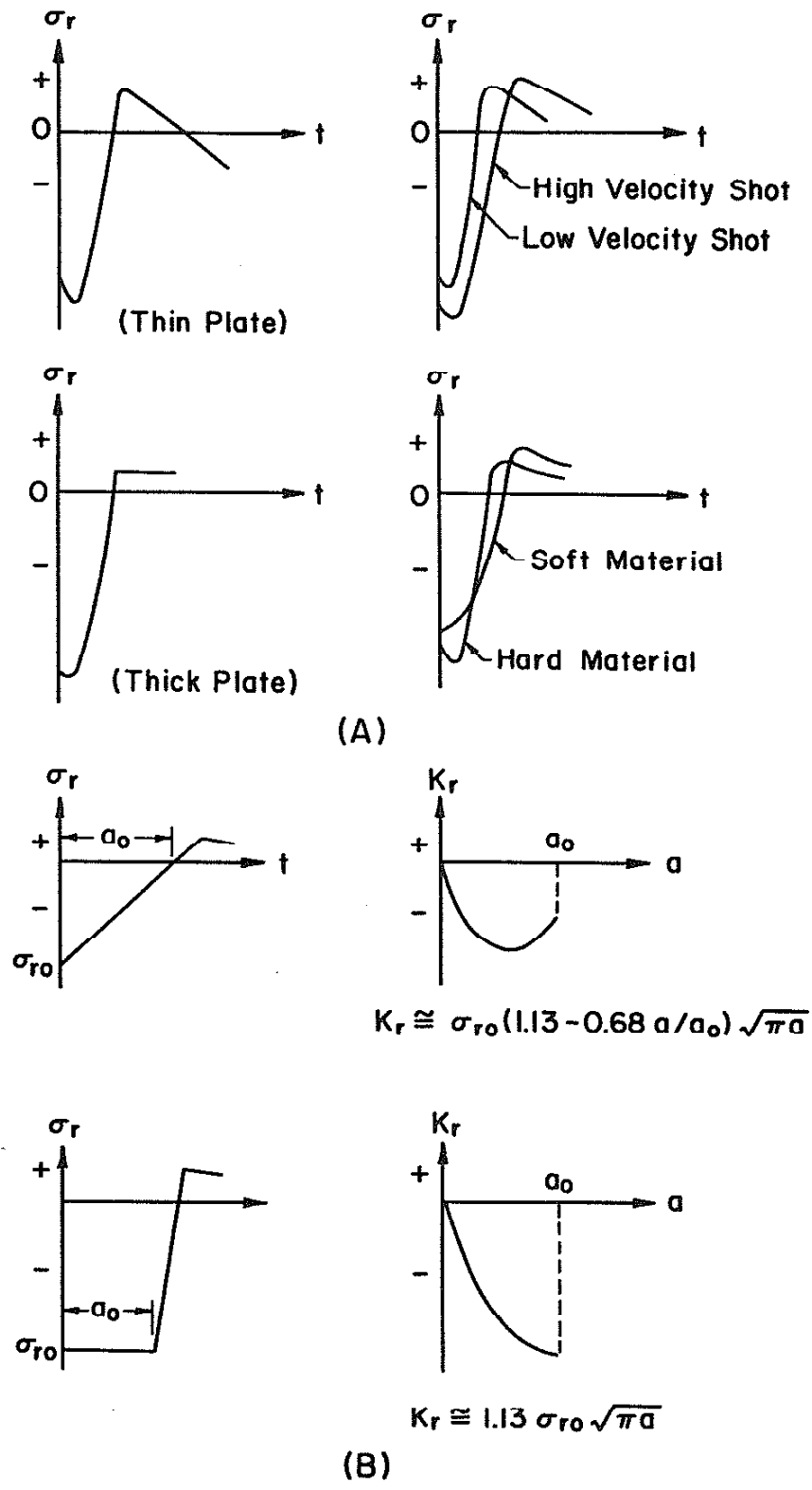


Fig. A2 (a) Typical residual stress distributions resulting from shot-peening [18]; (b) Hypothetical notch residual distributions and corresponding residual stress intensity factors [21,22].